



Cite this: *Catal. Sci. Technol.*, 2019, 9, 6492

Biomimetic catalytic oxidative coupling of thiols using thiolate-bridged dinuclear metal complexes containing iron in water under mild conditions†

Yahui Zhang,^a Dawei Yang,^a *^a Ying Li,^a Xiangyu Zhao,^a Baomin Wang,^a ^a and Jingping Qu *^{ab}

A green and efficient approach to disulfides *via* oxidative coupling of thiols was developed by adopting a biomimetic thiolate-bridged iron–ruthenium complex as the catalyst. Using environmentally friendly oxygen as the oxidant, a wide range of thiols including biologically important molecules can be smoothly converted into corresponding disulfides in water. Notably, two potential intermediate species were successfully isolated and unambiguously characterized, which is essential to reveal the detailed mechanism of this transformation. This catalytic system represents a rare and desired heteronuclear bimetallic scaffold for understanding the biological process of S–S bond formation from the viewpoint of bioinspired catalysis.

Received 19th August 2019,
Accepted 30th September 2019

DOI: 10.1039/c9cy01667h

rsc.li/catalysis

Introduction

Construction of the S–S bond is of great importance in numerous fields of chemistry and biology, because the resulting disulfides as structural linkers can play multifaceted roles.^{1–4} In biological proteins, the S–S bonds between cysteine residues can stabilize the native structure.^{1a} In drug development, disulfides as a vital component exhibit unique pharmacological activities such as anti-alcoholic^{2a} and anti-bacterial effects.^{2b} In addition, this crucial motif also extensively exists in natural products³ and food additives.⁴ In this context, great efforts had been made to develop efficient methods for the access to disulfides.⁵ Among these synthetic pathways, the oxidative coupling of thiols is the most effective strategy, especially for symmetrical disulfides. In fact, in recent decade, oxidative coupling between two nucleophiles catalyzed by transition metals has developed into an efficient approach for chemical bond formations, in which oxidants are usually involved.⁶ For example, to realize the formation of S–S bonds, various oxidants are generally required, such as oxygen or air,^{7,8} hydrogen peroxide,⁹ halogens,¹⁰ high-valent sulfur compounds¹¹ and other agents.¹² As people gradually become aware of environmental protection, the employment

of oxygen has attracted considerable attention from the synthetic community.¹³ Up to now, many homogeneous⁷ and heterogeneous⁸ catalytic systems containing transition-metal species utilizing oxygen have been successfully developed for the oxidative coupling of thiols. However, most of these cases usually have some obvious disadvantages including toxic solvents, high temperature, long reaction times, relatively low yields, and extra additives or bases. Therefore, the establishment of efficient, green, and sustainable methods for the formation of S–S bonds remains challenging and highly desirable.

In the past two decades, although several new strategies have been developed,¹⁴ the transition-metal catalyzed oxidative coupling of thiols to disulfides is still a most commonly used one. From the conventional view of metal catalysts, metal thiolate complexes usually play as inactive species in these catalytic cycles.¹⁵ However, the discovery of the active centres of various significant metalloenzymes in nature provides new understanding of the role of sulfur donors.¹⁶ Besides, the cooperative effect of bi- or multi-metallic sites is also essential to promote corresponding enzymatic activity.¹⁷ Nonetheless, there are no biomimetic systems for the catalytic oxidation of thiols to disulfides in aqueous medium reported. Furthermore, detailed mechanistic investigations by trapping potential intermediates using structural determination methods are less developed, despite these being helpful to obtain insights into biological processes involving S–S bond formation.

In our preliminary work, inspired by versatile metalloenzymes in biology, we were always devoted to constructing thiolate-bridged di- or multinuclear metal complexes for small molecule activation and transformation,

^a State Key Laboratory of Fine Chemicals, Dalian University of Technology, 2 Linggong Road, Dalian, 116024, P. R. China. E-mail: yangdw@dlut.edu.cn, qujp@dlut.edu.cn

^b Key Laboratory for Advanced Materials, East China University of Science and Technology, Shanghai, 200237, P. R. China

† Electronic supplementary information (ESI) available: Experimental and crystallographic details and spectral data. CCDC 1837831, 1837832, 1837835, 1843162, 1869211, 1869214 and 1869707. For ESI and crystallographic data in CIF or other electronic format see DOI: 10.1039/c9cy01667h

adopting different types of sulfur donors.^{18–20} Notably, several homo- and heterometallic thiolate complexes exhibit excellent catalytic properties by the cooperation effect.²¹ In order to further extend the catalytic performance of our reaction platforms, herein, we utilized the flexible thioether-dithiolate tridentate ligand tpdt (tpdt = S(CH₂CH₂S[−])₂) to prepare several tpdt-bridged heteronuclear complexes, among which an iron–ruthenium complex was proven to be an outstanding catalyst for the oxidation of mercaptans to disulfides in water employing oxygen as the oxidant at room temperature. Importantly, two potential intermediates during the catalytic cycle were fully characterized by X-ray crystallography.

Results and discussion

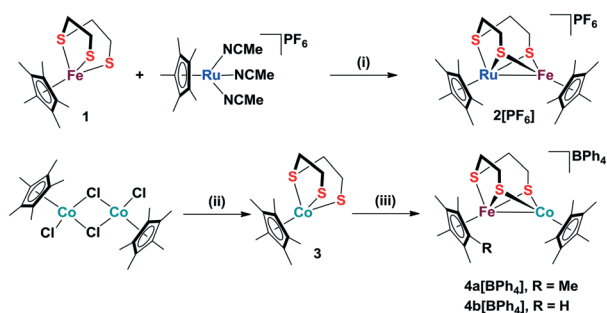
Synthesis of thiolate-bridged heterometallic complexes with iron

Our investigation was initiated by the construction of thioether-dithiolate-bridged heteronuclear metal complexes containing iron. As illustrated in Scheme 1, a tpdt-bridged iron–ruthenium complex [Cp^{*}Ru(μ-1-κ³SSS':2-κ²SS-tpdt)FeCp^{*}]₂[PF₆]₂ (2[PF₆], Cp^{*} = η⁵-C₅Me₅) was synthesized through the assembly of the two mononuclear precursors [Cp^{*}Ru(MeCN)₃][PF₆]²² and [Cp^{*}Fe(η³-tpdt)] (1)²³ in high yield. In view of mononuclear iron precursor 1 as a versatile building block²⁴ and reaction platform,²⁵ the mononuclear cobalt analogue [Cp^{*}Co(η³-tpdt)] (3) was synthesized by the interaction of [Cp^{*}Co(μ-Cl)₂(t-Cl)₂CoCp^{*}]²⁶ with 2 equiv. of Li₂(tpdt). Similarly, by adopting mononuclear cobalt complex 3 and [Cp^{*}Fe(MeCN)₃][PF₆]²⁷ as precursors, a similar iron–cobalt complex [Cp^{*}Fe(μ-1-κ³SSS':2-κ²SS-tpdt)CoCp^{*}][BPh₄] (4a[BPh₄]) was smoothly generated in good yield. To distinguish between iron and cobalt which have similar atomic radii, we also conducted a reaction employing [Cp[']Fe(MeCN)₃][PF₆] (Cp['] = η⁵-C₅Me₄H)²⁸ to facilitate the corresponding iron–cobalt complex [Cp[']Fe(μ-1-κ³SSS':2-κ²SS-tpdt)CoCp^{*}][BPh₄] (4b[BPh₄]).

These heteronuclear complexes were fully characterized by ¹H NMR, ¹³C NMR, ESI-HRMS, and IR spectroscopy as well as

elemental analysis. In the ¹H NMR spectrum of 2[PF₆], three remarkably broad proton resonances appear at −6.42, −0.64, and 3.03 ppm, which suggest that this iron–ruthenium complex should be a paramagnetic species. A similar phenomenon was also observed in other formal Fe^{II}Ru^{III} complexes.²⁹ Furthermore, solid evidence for the paramagnetism of 2[PF₆] was provided by other spectroscopic methods. Using Evans' method,³⁰ the effective magnetic susceptibility (μ_{eff}) of 2[PF₆] in solution was determined to be 1.77μ_B by ¹H NMR spectroscopy. In addition, the EPR spectrum of complex 2[PF₆] in the solid state at room temperature features a diagnostic signal at g = 2.07 (Fig. S2†). The above data indicate that complex 2[PF₆] is in an S = 1/2 spin state. Differently, iron–cobalt complexes 4a[BPh₄] and 4b[BPh₄] are all diamagnetic species confirmed by their ¹H NMR spectra, in which several intense resonances assignable to Cp^{*}, Cp['] and tpdt ligands appear in a common region. This result is attributed to the fact that cobalt has one more d electron than iron. In addition, their ¹³C NMR spectra were fully consistent with the aforementioned ¹H NMR results. Furthermore, electrospray ionization high resolution mass spectrometry (ESI-HRMS) was adopted to confirm the molecular compositions of these complexes. As expected, the corresponding molecular ion peaks for the cationic parts of complexes 2[PF₆], 4a[BPh₄] and 4b[BPh₄] were detected.

To get more structural information, these complexes were clearly determined by X-ray diffraction analysis, and the molecular structures of 2[PF₆] and 4b[BPh₄] are shown in Fig. 1 and 2, respectively. Their geometric arrangement is similar to that of the diiron analogue.²³ Interestingly, it is observable that the thioether sulfur atom in the bridging tpdt ligand flipped from the original metal center to the other one. This unusual phenomenon should be attributed to the flexibility of the tpdt ligand, because a similar situation is not observed when using other rigid tridentate ligands to construct heteronuclear complexes.³¹ In 2[PF₆], the Fe–Ru bond distance is 2.691(2) Å, which is very close to that of our other reported thiolate-bridged FeRu complex.²⁹ Because the thioether sulfur atom is coordinated to the ruthenium center, the interaction between the ruthenium center and bridging thiolate sulfur atoms is evidently weakened, which is



Scheme 1 Synthesis of heterometallic complexes 2[PF₆], 4a[BPh₄] and 4b[BPh₄]. Reagents and conditions: (i) MeCN, −45 °C to rt, 88%; (ii) 2 equiv. of Li₂(tpdt), THF, rt, 2 h, 55%; (iii) 1 equiv. of [Cp[']Fe(MeCN)₃][PF₆] (Cp['] = Cp^{*} or Cp[']), 1 equiv. of NaBPh₄, THF, −78 °C to rt, 82% for 4a[BPh₄], 83% for 4b[BPh₄].

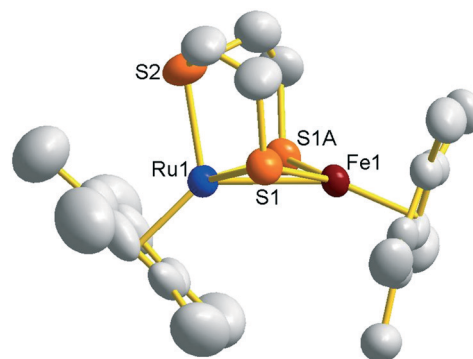


Fig. 1 Molecular structure of 2[PF₆] at 50% probability of ellipsoids. The PF₆ anion and hydrogen atoms are omitted for the sake of clarity.

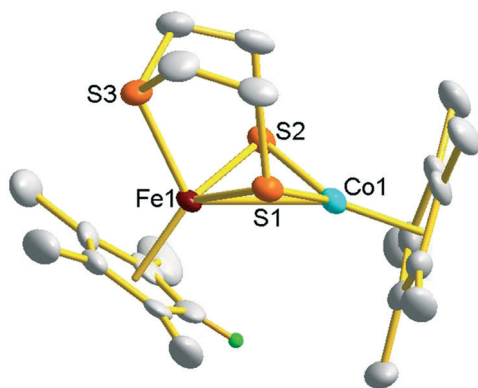


Fig. 2 Molecular structure of **4b**[BPh₄] at 50% probability of ellipsoids. The BPh₄ anion and hydrogen atoms except for the hydrogen atom on the Cp' ring are omitted for the sake of clarity.

consistent with the fact that the Ru1–S1 bond length of 2.305(2) Å is significantly longer than the Fe1–S1 bond length of 2.197(2) Å and almost equal to the Ru1–S2 bond length of 2.307(3) Å. In **4b**[BPh₄], to stabilize the coordinatively unsaturated iron center, the thioether sulfur atom occupies the remaining coordination site. A similar situation was also observed in the bidentate thiolate-bridged iron–cobalt complex [Cp*Co(μ-η²:η⁴-bdt)FeCp*][PF₆] (bdt = benzene-1,2-dithiolate).³² The minor substituent difference on the Cp rings of complexes **4a**[BPh₄] and **4b**[BPh₄] has a slight effect on the structural data. For example, the dihedral angles of two Cp rings in **4a**[BPh₄] is 66.78(21)°, which is smaller than 73.18(19)° in **4b**[BPh₄]. Besides, the Fe–Co bond distance of 2.6772(8) Å in **4a**[BPh₄] is slightly longer than 2.587(1) Å in **4b**[BPh₄]. These two bond lengths are located in a common range from 2.398(14) Å to 3.153(1) Å in reported dithiolate-bridged iron–cobalt complexes.³³

Aerobic oxidation of thiols catalysed by bimetallic complexes

Inspired by versatile catalytic properties mediated by heterometallic clusters in metalloenzymes and homogeneous

systems,^{17,34} we constructed heterometallic complexes to pursue the development of new systems for biomimetic catalysis. During our investigations about biomimetic oxidation using oxygen, we found that tpdt-bridged homo- or heterometallic complexes can serve as effective catalysts for the oxidative coupling of mercaptans. Based on this finding, a series of experiments were designed and performed.

At the outset, the catalytic transformation of thiophenol (**5a**) to diphenyl disulfide (**6a**) was selected as the model reaction to optimize the reaction conditions. For the sake of manifesting the unique catalytic nature of bimetallic complexes by the cooperation effect, several mononuclear precursor complexes were chosen as catalysts. In addition, to understand the differences of metal centres in catalytic activity, diiron and nickel–iron analogues of complex **2**[PF₆] were also examined. All experimental results are summarized in Table 1 (the detailed coordination modes of the bridging tpdt ligand are simplified due to space constraints of the table).

In the presence of 1 mol% catalyst, the mononuclear iron, ruthenium, and cobalt complexes show poor activity for the oxidative coupling of thiols in THF-*d*₈ at room temperature under an oxygen atmosphere (entries 1–5). Notably, when the three labile MeCN groups were replaced by the tridentate tpdt ligand, the conversion and yield significantly increased, especially with mononuclear iron and cobalt complexes **1** and **3** (entries 3 and 5). To our delight, when the tpdt-bridged diiron complex [Cp*Fe(μ-1,3^{SSS'}:2^κSS-pdt)FeCp*][PF₆] was adopted as the catalyst, a high conversion and yield were obtained as shown in entry 6. Nonetheless, iron–nickel complex [Cp*Fe(μ-tpdt)Ni(dppe)][PF₆] and iron–cobalt complex **4a**[BPh₄] with a similar core structure were proven to be poor promoters for the conversion of thiophenol to diphenyl sulfide (entries 7 and 9). In addition, iron–ruthenium complex **2**[PF₆] can also serve as an excellent catalyst with a high conversion and yield similar to its diiron analogue (entry 8). Essentially, its binuclear reaction scaffold still remains after catalytic transformation, which is different from the diiron complex. As observed, [Cp*Fe(μ-1,3^{SSS'}:2^κSS-

Table 1 Aerobic oxidation of thiophenol to diphenyl disulfide catalyzed by various mono- and dinuclear metal complexes^a

Entry	Catalyst	2 PhSH $\xrightarrow[\text{under O}_2 \text{ atmosphere}]{\text{Cat. (1 mol\%)}} \text{PhSSPh}$	
		THF- <i>d</i> ₈ , rt, 15 min,	
		Conversion ^b (%)	Yield ^b (%)
1	[Cp*Fe(MeCN) ₃][PF ₆]	16	9
2	[Cp*Ru(MeCN) ₃][PF ₆]	16	12
3	[Cp*Fe(η ³ -tpdt)]	74	71
4	[Cp*Ru(η ³ -tpdt)]	33	31
5	[Cp*Co(η ³ -tpdt)]	68	66
6	[Cp*Fe(μ-tpdt)FeCp*][PF ₆]	100	93
7	[Cp*Fe(μ-tpdt)Ni(dppe)][PF ₆]	36	34
8	2 [PF ₆]	100	95
9	4a [BPh ₄]	20	11

^a Reaction conditions: thiophenol (1.8 mmol), catalyst (0.018 mmol, 1 mol%), THF-*d*₈ (0.6 mL), under an O₂ atmosphere, rt, 15 min. ^b The yield and conversion were determined by ¹H NMR spectroscopy with hexamethylbenzene as an internal standard.

pdT)FeCp*][PF₆] was almost completely decomposed into unidentified insoluble species after the catalytic reaction was completed.

Moreover, we also explored the solvent effects in the conversion and yield of this reaction. The screening results show that THF is the optimal solvent (Table S1†). Furthermore, the loading of catalyst 2[PF₆] was also investigated from 1 mol% to 0.1 mol%. As a result, 1 mol% catalyst was required for the accomplishment of this catalytic process, which is evidenced by the fact that the obvious decrease of the yield is accompanied with the reduction of the amount of catalyst (Table S2†). Besides, control experiments have also been implemented to demonstrate the importance of the compatibility between catalyst and oxidant. One step further, we have also tried the synthesis of unsymmetrical disulfides through the oxidative cross coupling of different thiols catalyzed by complex 2[PF₆] under similar conditions. Formation of unsymmetrical disulfides was observed, but the selectivity is moderate due to the appearance of homo-coupling products.

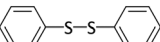
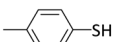
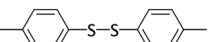
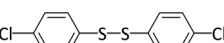
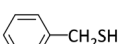
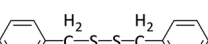
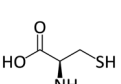
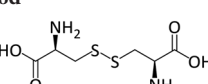
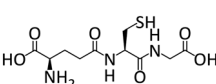
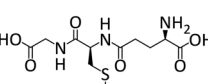
From the viewpoints of environmental and sustainable prospects,³⁵ we sought to develop a greener catalytic system for the synthesis of disulfides. To achieve this aim, we attempted to utilize water as the solvent, replacing THF. Delightedly, the oxidative coupling of thiophenol catalyzed by 2[PF₆] smoothly proceeded in water, although it is necessary to extend the reaction time to 3 h for complete conversion.

Under the green and mild conditions, we next examined the substrate scope of this oxidation reaction using 2[PF₆] (1 mol%) as the catalyst. As shown in Table 2, complex 2[PF₆] was proven to be an efficient catalyst with good functional group compatibility for oxidative coupling of thiols to corresponding disulfides. For instance, thiophenol derivatives (5b and 5c) bearing electron-donating and electron-withdrawing groups at the *para* positions on the phenyl ring can readily be oxidized to afford the corresponding disulfides (6b and 6c) in high yields. In addition, benzyl mercaptan (5d) as a representative aliphatic thiol was also oxidized to generate disulfide 6d in good yield. Furthermore, conversion of some biological relevant organosulfur compounds such as cysteine (5e) and reduced glutathione (5f) into cystine (6e) and oxidized glutathione (6f), respectively, were also realized in high yields. The achievement of these two cases provides a new biomimetic reaction platform in aqueous medium for obtaining more insights into peptide bond formation in cells.

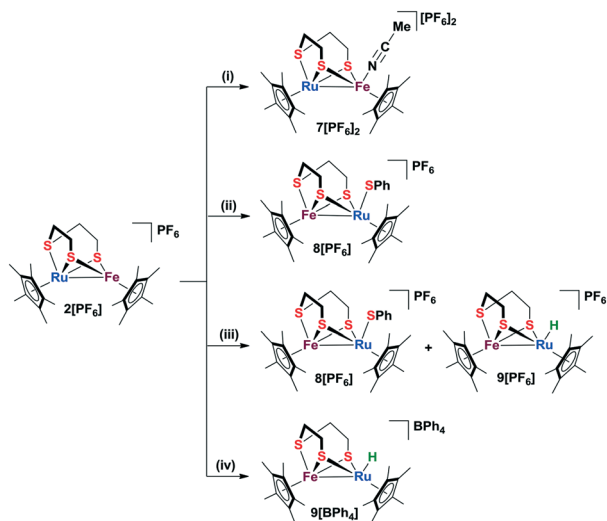
Mechanistic considerations

To get a deep insight into plausible reaction pathways of the catalytic oxidation of thiols using 2[PF₆], a series of experiments were conducted to corroborate potential intermediate species. Also, thiophenol was selected as a representative substrate for mechanistic studies. Firstly, we

Table 2 Oxidation of thiols catalyzed by 2[PF₆]^a

Entry	Thiol	Disulfide	Yield ^b (%)
1	 5a	 6a	90
2	 5b	 6b	90
3	 5c	 6c	89
4	 5d	 6d	82
5	 5e	 6e	97
6	 5f	 6f	94

^a Reaction conditions: thiol (1.8 mmol), 2[PF₆] (0.018 mmol, 1 mol%), H₂O (2 mL), under an O₂ atmosphere, rt, 3 h. ^b Isolated yields.



Scheme 2 Synthesis of complexes 7[PF₆]₂, 8[PF₆] and 9[BPh₄]. Reagents and conditions: (i) air, MeCN, rt, 1 h, 42%; (ii) ex. PhSH, O₂ (1 atm), THF, rt, 15 min, 88%; (iii) ex. PhSH, THF, rt, 15 min; (iv) 1 equiv. of CoCp₂, 1 equiv. of Lut-HBPh₄, 1 equiv. of NaBPh₄, THF, -78 °C to rt, 85%.

explored the reactivity of complex 2[PF₆] towards one atmosphere of oxygen in the absence of thiophenol. Complex 2[PF₆] was robust under an inert atmosphere whether in solution or the solid state. However, when a THF solution of complex 2[PF₆] was exposed to oxygen for about 1 h, further oxidized product 2[PF₆]₂ was detected by ESI-MS analysis, accompanied with a great deal of precipitates. This result indicates that a disproportionation process of 2[PF₆] may occur, promoted by oxygen. However, the reaction selectivity is too poor to conduct further isolation and purification of complex 2[PF₆]₂. With weakly coordinative MeCN as the solvent, an expected dicationic Fe^{III}Ru^{III} complex [Cp*₂Fe(μ-1,3-SSS':2,2'-SS-tpdt){Cp*Ru(t-MeCN)}][PF₆]₂ (7[PF₆]₂) can be successfully isolated in moderate yield (Scheme 2). Independently, complex 7[PF₆]₂ can also be obtained by the reaction of 2[PF₆] with one-electron oxidant Fc-PF₆ in MeCN.

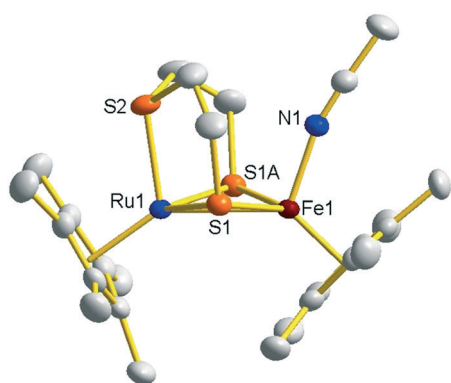


Fig. 3 Molecular structure of 7[PF₆]₂ at 50% probability of ellipsoids. The two PF₆ anions and hydrogen atoms are omitted for the sake of clarity.

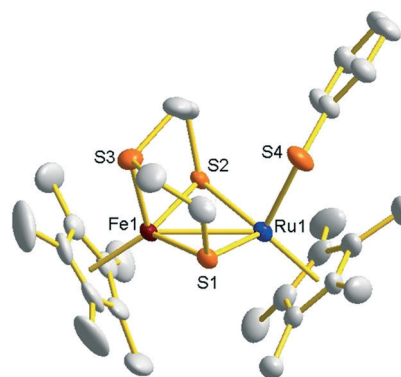


Fig. 4 Molecular structure of 8[PF₆] at 50% probability of ellipsoids. The PF₆ anion and hydrogen atoms are omitted for the sake of clarity.

The ¹H NMR spectrum of 7[PF₆]₂ shows four sets of proton resonances for the four inequivalent methylene groups in the tpdt ligand and two intense singlets for the methyl groups of two inequivalent Cp* groups. All assignments of ¹H NMR data are fully consistent with the structural information determined from the ¹³C NMR spectrum of 7[PF₆]₂. Crystallographic analysis shows that one MeCN molecule occupies the open coordination site (see Fig. 3). The Fe–Ru distance in 7[PF₆]₂ is slightly lengthened from 2.691(2) Å in 2[PF₆] to 2.794(2) Å.

Subsequently, under aerobic conditions, the reaction of 2[PF₆] with a slight excess of thiophenol gave the only product [Cp*₂Fe(μ-1,3-SSS':2,2'-SS-tpdt){Cp*Ru(t-SPh)}][PF₆] (8[PF₆]) in good yield (Scheme 2). Oxidation of 2[PF₆] to form a dicationic species was not observed. Complex 8[PF₆] was unambiguously characterized by spectroscopy and crystallography. Interestingly, the crystal structure shown in Fig. 4 reveals that the pendent thioether sulfur atom in the tpdt ligand returned from the ruthenium center to the iron center. Meanwhile, a phenylthiolate group was coordinated to the ruthenium centre.

Interestingly, treatment of 2[PF₆] with an excess of thiophenol in THF-*d*₈ under anaerobic conditions gave a mixture of complex 8[PF₆] and terminal hydride complex [Cp*₂Fe(μ-1,3-SSS':2,2'-SS-tpdt){Cp*Ru(t-H)}][PF₆] (9[PF₆]), identified using the ¹H NMR spectrum and ESI-HRMS data.

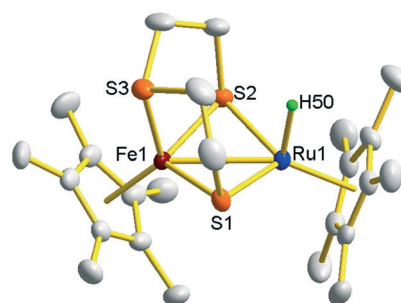


Fig. 5 Molecular structure of 9[BPh₄] at 50% probability of ellipsoids. The BPh₄ anion and hydrogen atoms except the terminal hydride are omitted for the sake of clarity.

Due to the restriction of coordination number, the phenylthiolate and hydride groups derived from thiophenol didn't bind to the same bimetallic scaffold through an oxidative addition fashion as in other metallic systems.³⁶ In the ¹H NMR spectrum, four sharp peaks appear at 1.60, 1.68, 1.71 and 1.93 ppm, assignable to two sets of inequivalent Cp* methyl proton signals of complexes **8**[PF₆] and **9**[PF₆], respectively (Fig. S18[†]). In addition, a diagnostic signal for the terminal hydride appears at -16.81 ppm in the high field region, which is close to -16.44 ppm of a phosphine-dithiolate-bridged diruthenium terminal hydride complex,³⁷ but is significantly located in a higher field than those of other thiolate-bridged diruthenium complexes.^{36a,38} In addition, the terminal hydride complex **8**[PF₆] can also be independently generated through the reductive protonation of **2**[PF₆] in excellent yield (Scheme 2).

Single-crystals suitable for X-ray diffraction analysis were obtained by further counter ion exchange. As shown in Fig. 5, the molecular structure of **9**[BPh₄] reveals a hydride ligand terminally coordinated to the ruthenium center accompanied with shifting of the pendant thioether sulfur atom to the iron center. These structural variations cause the Fe–Ru distance of 2.7411(4) Å in **9**[BPh₄] to be slightly lengthened compared with 2.691(2) Å in **2**[PF₆]. Interestingly, different from bdt-bridged bimetallic systems,²⁹ the terminal hydride complex **9**[BPh₄] is relatively insensitive to temperature and is stable under an inert atmosphere at room temperature.

In order to test the identity of potential intermediates, we carried out the catalytic oxidation of thiophenol with these complexes. Due to its insolubility in THF, complex **7**[PF₆]₂ was firstly excluded as a potential intermediate species. However, complex **8**[PF₆] can serve as an excellent catalyst for oxidative coupling of thiols to disulfides under an O₂ atmosphere (Table S4[†]). In addition, **9**[BPh₄] was also proven to be an effective catalyst for oxidation of thiols under similar conditions, in spite of its relatively low efficiency compared with **8**[PF₆]. This result can be explained by the instability of **9**[BPh₄] in the presence of excess substrates under an O₂ atmosphere. Realization of this catalytic reaction promoted by these two complexes suggests that they should function as essential intermediates during this catalytic process.

Based on the above results and previous reports for the pathways of this type of reaction,^{8d} a proposed mechanism of

this oxidation process is shown in Scheme 3. Firstly, catalyst **2**[PF₆] interacts with thiols to simultaneously generate complexes **8**[PF₆] and **9**[PF₆], which is strongly supported by the above experimental results. Then, these two complexes can transform into initial species **2**[PF₆] through two different pathways. In the left semicircle, complex **8**[PF₆] converts into **2**[PF₆] in the presence of a thiol and oxygen accompanied with the release of the oxidation product PhSSPh and side-product H₂O. Meanwhile, in the right semicircle, the intermediate **9**[PF₆] reduces molecular oxygen to give H₂O along with the regeneration of complex **2**[PF₆]. The two sections combine together to accomplish a catalytic cycle. Finally, the main residue containing metals in solution was complex **8**[PF₆], which cannot further release disulfides through the left semicircle due to exhaustion of thiophenol.

Conclusions

In summary, several thiolate-bridged heteronuclear complexes containing iron were successfully synthesized by an assembly reaction and fully characterized by spectroscopy and crystallography. Iron–ruthenium complex **2**[PF₆] can serve as an excellent catalyst for oxidation of thiols to symmetrical disulfides employing environmentally friendly oxygen in aqueous medium at room temperature. Unexpectedly, this green method is not only applicable to common organic thiols, but also to small molecules with biological significance such as cysteine and reduced glutathione. Achievement of this bio-inspired oxidation by the bimetallic cooperative effect is conducive to gain new insights into some important biological processes involving S–S bond formation. Furthermore, two potential intermediates in the catalytic cycle were unambiguously characterized by X-ray diffraction analysis, which provides vital evidence for the detailed elucidation of the reaction mechanism. Studies on other potential catalytic oxidation processes and biological activities are now in progress.

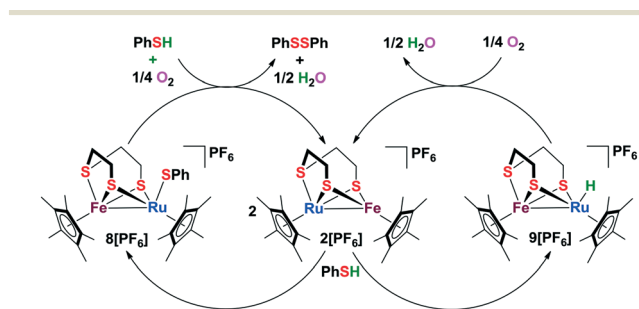
Experimental section

General procedures

All manipulations were carried out under a dry argon atmosphere by using standard Schlenk techniques and a Mikrouna argon-filled glove box. All solvents were dried and distilled over an appropriate drying agent under argon. pentamethylcyclopentadiene (Cp*H),³⁹ Lut-HBPh₄,⁴⁰ Fc-PF₆,⁴¹ [Cp*Ru(MeCN)₃][PF₆],²² [Cp*Fe(η³-tpdt)] (1),²³ [Cp*Co(μ-Cl)₂(t-Cl)₂CoCp*],²⁶ [Cp*Fe(MeCN)₃][PF₆],²⁷ [Cp*Fe(MeCN)₃][PF₆]²⁸ and [Cp*Ru(η³-tpdt)]⁴² were prepared according to literature procedures. RuCl₃ (Aldrich), anhydrous FeCl₂ (Aldrich), S(CH₂CH₂SH)₂ (Aldrich), NaBPh₄ (Energy Chemical), CoCp₂ (Energy Chemical), and mercaptans (Energy Chemical) were used as received without further purification.

Spectroscopic measurements

Infrared spectra were recorded on a NEXVSTM FT-IR spectrometer. Elemental analyses were performed using a



Scheme 3 Plausible catalytic mechanism for the **2**[PF₆]-catalyzed oxidation of thiols to disulfides with molecular oxygen as an oxidant.

Vario EL analyzer. The ^1H and ^{13}C NMR spectra were recorded on a Bruker 400 Ultra Shield spectrometer. The chemical shifts (δ) are given in parts per million relative to CD_3CN (1.94 ppm for ^1H ; 118.26 ppm for ^{13}C), CD_2Cl_2 (5.32 ppm for ^1H ; 53.84 ppm for ^{13}C), CDCl_3 (7.26 ppm for ^1H , 77.16 ppm for ^{13}C), C_6D_6 (7.16 ppm for ^1H , 128.06 ppm for ^{13}C), $\text{THF}-d_8$ (1.72, 3.58 ppm for ^1H), and D_2O (4.79 ppm for ^1H). ESI-HRMS data were recorded on an HPLC/Q-ToF mass spectrometer. The EPR spectra were recorded at room temperature on a JEOL JES-FE3AX spectrometer.

X-ray crystallography procedures

The data were obtained on a Bruker SMART APEX CCD diffractometer with graphite monochromated Mo $K\alpha$ radiation ($\lambda = 0.71073 \text{ \AA}$). Empirical absorption corrections were performed using the SADABS program.⁴³ Structures were solved by direct methods and refined by the full-matrix least-squares method based on all data using F^2 with SHELX2014.⁴⁴ All of the non-hydrogen atoms were refined anisotropically. All of the hydrogen atoms were generated and refined in ideal positions.

One CH_2 group in the tpdt ligand of complex $2[\text{PF}_6]$ and one CH_2 group in the tpdt ligand of complex $7[\text{PF}_6]_2$ were disordered and restrained during structural refinement. Disordered atomic positions were split and refined using one occupancy parameter per disordered group. We used SQUEEZE to help us solve the level B alert of solvent accessible voids when checking the cif file of $9[\text{BPh}_4]$ through CheckCIF (<http://checkcif.iucr.org>). Crystal data and collection details for $2[\text{PF}_6]$ and 3 are given in Table S6;† crystal data and collection details for $4a[\text{BPh}_4]$ and $4b[\text{BPh}_4]$ are given in Table S7;† crystal data and collection details for $7[\text{PF}_6]_2$, $8[\text{PF}_6]$, and $9[\text{BPh}_4]$ are given in Table S8.†

Synthesis of $[\text{Cp}^*\text{Ru}(\mu\text{-}1_{\kappa^3}\text{SSS}':2_{\kappa^2}\text{SS-tpdt})\text{FeCp}^*][\text{PF}_6]$ ($2[\text{PF}_6]$). A solution of $[\text{Cp}^*\text{Fe}(\eta^3\text{-tpdt})]$ (1 , 161 mg, 0.47 mmol) in MeCN (15 mL) was cooled to -45°C . Then, a solution of $[\text{Cp}^*\text{Ru}(\text{MeCN})_3][\text{PF}_6]$ (237 mg, 0.47 mmol) in MeCN (20 mL) at -45°C was transferred *via* a cannula to the cooled solution of 1 . The mixture was stirred overnight as it warmed to room temperature. The resulting yellow-green solution was evaporated and washed with Et_2O ($3 \times 10 \text{ mL}$). The product, $[\text{Cp}^*\text{Ru}(\mu\text{-}1_{\kappa^3}\text{SSS}':2_{\kappa^2}\text{SS-tpdt})\text{FeCp}^*][\text{PF}_6]$ ($2[\text{PF}_6]$, 300 mg, 0.41 mmol, 88%), was obtained as a yellow-green crystalline powder. Crystals suitable for X-ray diffraction were obtained from a THF solution layered with *n*-hexane at room temperature. ^1H NMR (400 MHz, CD_3CN , ppm): δ -6.42 (br), -0.64 (s), 3.03 (s). μ_{eff} (CD_3CN , Evans' method, 25°C) = $1.77\mu_{\text{B}}$. ESI-HRMS (m/z): calcd. for 2^+ : 580.0535; found: 580.0549. IR (film, cm^{-1}): 2962, 2852, 1379, 1021, 558. EPR (298 K): $g = 2.07$. Anal. calcd. for $\text{C}_{24}\text{H}_{38}\text{FeRuS}_3\text{PF}_6$: C, 39.78; H, 5.29. Found: C, 39.56; H, 4.99.

Synthesis of $[\text{Cp}^*\text{Co}(\eta^3\text{-tpdt})]$ (3). At room temperature, a suspension of $\text{Li}_2(\text{tpdt})$ in THF (30 mL), prepared by the reaction of $n\text{-BuLi}$ (3.02 mL, 2.5 M solution in *n*-hexane, 7.56 mmol) and $\text{S}(\text{CH}_2\text{CH}_2\text{SH})_2$ (580 mg, 3.78 mmol) at 0°C , was

transferred *via* a cannula to a THF (30 mL) solution of $[\text{Cp}^*\text{Co}(\mu\text{-Cl})_2(\text{t-Cl})_2\text{CoCp}^*]$ (1.00 g, 1.89 mmol) and the mixture was stirred for 2 h, resulting in a violet solution. All volatiles were removed *in vacuo* and the residue was extracted with *n*-hexane ($3 \times 100 \text{ mL}$). After being cooled to -30°C for one day, black thin slice crystals of $[\text{Cp}^*\text{Co}(\eta^3\text{-tpdt})]$ (3 , 720 mg, 2.08 mmol, 55%) were isolated. ^1H NMR (400 MHz, C_6D_6 , ppm): δ 1.40 (s, 15H, $\text{Cp}^*\text{-CH}_3$), 1.82 (m, 4H, tpdt-CH_2), 2.13 (m, 4H, tpdt-CH_2). ^{13}C NMR (100 MHz, C_6D_6 , ppm): δ 9.29 ($\text{Cp}^*\text{-CH}_3$), 30.70 (SCH_2), 45.95 (SCH_2), 93.17 ($\text{Cp}^*\text{-C}$). IR (film, cm^{-1}): 2960, 2905, 1428, 1372, 1095, 1022, 832. Anal. calcd. for $\text{C}_{14}\text{H}_{23}\text{CoS}_3$: C, 48.54; H, 6.69. Found: C, 48.26; H, 6.64.

Synthesis of $[\text{Cp}^*\text{Fe}(\mu\text{-}1_{\kappa^3}\text{SSS}':2_{\kappa^2}\text{SS-tpdt})\text{CoCp}^*][\text{BPh}_4]$ ($4a[\text{BPh}_4]$). At -78°C , a solution of $[\text{Cp}^*\text{Fe}(\text{MeCN})_3][\text{PF}_6]$ (165 mg, 0.36 mmol) in THF (20 mL) was added to a THF (20 mL) mixed solution of 3 (125 mg, 0.36 mmol) and NaBPh_4 (123 mg, 0.36 mmol). Then, the resulting solution was stirred vigorously as it warmed to room temperature, resulting in a brown-red solution. Then, the supernatant solution was filtered and evaporated to dryness in a vacuum. The resulting product, $[\text{Cp}^*\text{Fe}(\mu\text{-}1_{\kappa^3}\text{SSS}':2_{\kappa^2}\text{SS-tpdt})\text{CoCp}^*][\text{BPh}_4]$ ($4a[\text{BPh}_4]$, 257 mg, 0.30 mmol, 82%), was obtained as a brown powder. Crystals suitable for X-ray diffraction were obtained from a CH_2Cl_2 solution layered with *n*-hexane at room temperature. ^1H NMR (400 MHz, CD_2Cl_2 , ppm): δ 1.20 (s, 15H, $\text{Cp}^*\text{-CH}_3$), 1.67 (m, 2H, tpdt-CH_2), 2.04 (m, 2H, tpdt-CH_2), 2.53 (s, 15H, $\text{Cp}^*\text{-CH}_3$), 2.68 (m, 2H, tpdt-CH_2), 4.26 (m, 2H, tpdt-CH_2), 6.87 (m, 4H, Ph-*H*), 7.02 (m, 8H, Ph-*H*), 7.31 (m, 8H, Ph-*H*). ^{13}C NMR (100 MHz, CD_2Cl_2 , ppm): δ 9.10 ($\text{Cp}^*\text{-CH}_3$), 10.50 ($\text{Cp}^*\text{-CH}_3$), 40.30 (SCH_2), 44.69 (SCH_2), 95.96 ($\text{Cp}^*\text{-C}$), 99.56 ($\text{Cp}^*\text{-C}$), 122.13 (Ph-*C*), 126.02 (Ph-*C*), 136.31 (Ph-*C*). ESI-HRMS (m/z): calcd. for $4a^+$: 537.0817; found: 537.0803. IR (film, cm^{-1}): 3052, 2962, 2851, 1579, 1478, 1090, 1201, 733, 705, 607. Anal. calcd. for $\text{C}_{48}\text{H}_{58}\text{BCoFeS}_3$: C, 67.29; H, 6.82. Found: C, 67.54; H, 6.90.

Synthesis of $[\text{Cp}'\text{Fe}(\mu\text{-}1_{\kappa^3}\text{SSS}':2_{\kappa^2}\text{SS-tpdt})\text{CoCp}^*][\text{BPh}_4]$ ($4b[\text{BPh}_4]$). At -78°C , a solution of $[\text{Cp}'\text{Fe}(\text{MeCN})_3][\text{PF}_6]$ (142 mg, 0.32 mmol) in THF (20 mL) was added to a THF (20 mL) mixed solution of 3 (111 mg, 0.32 mmol) and NaBPh_4 (109 mg, 0.32 mmol). Then, the resulting solution was stirred vigorously as it warmed to room temperature, resulting in a brown-red solution. Then, the supernatant solution was filtered and evaporated to dryness in a vacuum. The resulting product, $[\text{Cp}'\text{Fe}(\mu\text{-}1_{\kappa^3}\text{SSS}':2_{\kappa^2}\text{SS-tpdt})\text{CoCp}^*][\text{BPh}_4]$ ($4b[\text{BPh}_4]$, 227 mg, 0.27 mmol, 83%), was obtained as a brown powder. Crystals suitable for X-ray diffraction were obtained from a CH_2Cl_2 solution layered with *n*-hexane at room temperature. ^1H NMR (400 MHz, CD_2Cl_2 , ppm): δ 1.21 (s, 6H, $\text{Cp}'\text{-CH}_3$), 1.84 (s, 15H, $\text{Cp}^*\text{-CH}_3$), 1.87 (s, 6H, $\text{Cp}'\text{-CH}_3$), 2.48 (m, 4H, tpdt-CH_2), 3.10 (m, 4H, tpdt-CH_2), 3.92 (s, 1H, $\text{Cp}'\text{-H}$), 6.85 (m, 4H, Ph-*H*), 7.00 (m, 8H, Ph-*H*), 7.28 (m, 8H, Ph-*H*). ^{13}C NMR (100 MHz, CD_2Cl_2 , ppm): δ 10.41 ($\text{Cp}'\text{-CH}_3$), 11.15 ($\text{Cp}^*\text{-CH}_3$), 11.31 ($\text{Cp}'\text{-CH}_3$), 35.95 (SCH_2), 47.54 (SCH_2), 72.62 ($\text{Cp}'\text{-C}$), 91.37 ($\text{Cp}^*\text{-C}$), 97.95 ($\text{Cp}'\text{-C}$), 98.42 ($\text{Cp}'\text{-C}$), 122.53 (Ph-*C*), 126.59 (Ph-*C*), 136.65 (Ph-*C*). ESI-HRMS (m/z):

calcd. for **4b**⁺: 523.0661; found: 523.0658. IR (film, cm⁻¹): 3051, 2913, 2851, 1579, 1478, 1426, 1096, 1020, 804, 705, 607. Anal. calcd. for C₄₈H₅₈BCoFeS₃: C, 66.99; H, 6.70. Found: C, 66.92; H, 6.68.

Synthesis of [CpRu*(μ-1_κ³SSS':2_κ²SS-tpdt){Cp**Fe*(t-MeCN)}][PF₆]₂ (7[PF₆]₂).** Method A: A solution of 2[PF₆] (152 mg, 0.21 mmol) in MeCN (20 mL) was stirred at room temperature, exposing to air for 1 h. During this time, the colour gradually changed from yellow-green to brown-yellow. After removal of the volatiles under reduced pressure, the yellow residue was washed with Et₂O (3 × 10 mL) to afford crystalline solids of [Cp**Ru*(μ-1_κ³SSS':2_κ²SS-tpdt){Cp**Fe*(t-MeCN)}][PF₆]₂ (7[PF₆]₂, 80 mg, 0.09 mmol, 42%). Method B: Fc·PF₆ (70 mg, 0.21 mmol) was added to a yellow-green MeCN (20 mL) solution of 2[PF₆] (152 mg, 0.21 mmol) and the mixture was stirred at room temperature for 1 h. The resulting brown-yellow solution was evaporated, and then the residue was washed with Et₂O (3 × 10 mL) to remove the Fc by-product. The resulting product, [Cp**Ru*(μ-1_κ³SSS':2_κ²SS-tpdt){Cp**Fe*(t-MeCN)}][PF₆]₂ (7[PF₆]₂, 173 mg, 0.19 mmol, 90%), was obtained as a yellow powder after drying *in vacuo*. Crystals suitable for X-ray diffraction were obtained from a MeCN solution layered with Et₂O at room temperature. ¹H NMR (400 MHz, CD₃CN, ppm): δ 1.51 (s, 15H, Cp*-CH₃), 1.81 (s, 15H, Cp*-CH₃), 1.95 (s, 3H, CH₃CN), 2.18 (m, 2H, tpdt-CH₂), 2.74 (m, 2H, tpdt-CH₂), 2.92 (m, 2H, tpdt-CH₂), 3.40 (m, 2H, tpdt-CH₂). ¹³C NMR (100 MHz, CD₃CN, ppm): δ 10.49 (Cp*-CH₃), 10.89 (Cp*-CH₃), 38.40 (SCH₂), 40.28 (SCH₂), 103.17 (Cp*-C), 106.17 (Cp*-C). ESI-HRMS (*m/z*): calcd. for 7²⁺: 290.0268; found: 290.0259. IR (film, cm⁻¹): 2972, 2922, 1484, 1380, 1269, 1020, 837, 736, 558. Anal. calcd. for C₂₆H₄₁FeRuS₃NP₂F₁₂: C, 34.29; H, 4.54; N, 1.54. Found: C, 34.48; H, 4.30; N, 1.42.

Synthesis of [CpFe*(μ-1_κ³SSS':2_κ²SS-tpdt){Cp**Ru*(t-SPh)}][PF₆] (8[PF₆]).** To a stirred suspension of 2[PF₆] (123 mg, 0.17 mmol) in THF (10 mL), thiophenol (60 μL, 0.58 mmol) was added at room temperature, and the mixture was stirred under an O₂ atmosphere for 15 min. Then, the solution was evaporated to dryness under reduced pressure. The residue was washed with Et₂O (3 × 10 mL) to give a yellow product [Cp**Fe*(μ-1_κ³SSS':2_κ²SS-tpdt){Cp**Ru*(t-SPh)}][PF₆] (8[PF₆], 125 mg, 0.15 mmol, 88%). Crystals suitable for X-ray diffraction were obtained from a THF solution layered with *n*-hexane at room temperature. ¹H NMR (400 MHz, CD₃CN, ppm): δ 1.64 (s, 15H, Cp*-CH₃), 1.66 (s, 15H, Cp*-CH₃), 2.69 (m, 2H, tpdt-CH₂), 2.80 (m, 2H, tpdt-CH₂), 3.12 (m, 4H, tpdt-CH₂), 6.84 (m, 1H, Ph-*H*), 7.00 (m, 2H, Ph-*H*), 7.05 (m, 2H, Ph-*H*). ¹³C NMR (100 MHz, CD₃CN, ppm): δ 10.49 (Cp*-CH₃), 10.78 (Cp*-CH₃), 38.72 (SCH₂), 38.80 (SCH₂), 100.65 (Cp*-C), 104.18 (Cp*-C), 122.45 (Ph-C), 128.22 (Ph-C), 132.19 (Ph-C). ESI-HRMS (*m/z*): calcd. for 8⁺: 689.0648; found: 689.0656. IR (film, cm⁻¹): 2964, 2858, 1576, 1471, 1377, 1067, 841, 558. Anal. calcd. for C₃₀H₄₃FeRuS₄PF₆: C, 43.22; H, 5.20. Found: C, 43.48; H, 5.06.

Synthesis of [CpFe*(μ-1_κ³SSS':2_κ²SS-tpdt){Cp**Ru*(t-H)}][BPh₄] (9[BPh₄]).** At -78 °C, a solution of CoCp₂ (32 mg, 0.17

mmol) in THF (10 mL) was added to a THF (20 mL) mixed solution of 2[PF₆] (123 mg, 0.17 mmol), Lut·HBPh₄ (73 mg, 0.17 mmol) and NaBPh₄ (58 mg, 0.17 mmol). The reaction mixture was warmed to room temperature, resulting in a brown-yellow solution. The supernatant solution was filtered and evaporated to dryness under reduced pressure. The residue was washed with Et₂O (3 × 10 mL) and a yellow powder of [Cp**Fe*(μ-1_κ³SSS':2_κ²SS-tpdt){Cp**Ru*(t-H)}][BPh₄] (9[BPh₄], 130 mg, 0.14 mmol, 85%) was obtained. Crystals suitable for X-ray diffraction were obtained from a THF solution layered with *n*-hexane at room temperature. ¹H NMR (400 MHz, CD₃CN, ppm): δ -16.95 (s, 1H, Ru-*H*), 1.56 (s, 15H, Cp*-CH₃), 1.90 (s, 15H, Cp*-CH₃), 2.13 (m, 2H, tpdt-CH₂), 2.39 (m, 2H, tpdt-CH₂), 2.63 (m, 2H, tpdt-CH₂), 3.17 (m, 2H, tpdt-CH₂), 6.84 (m, 4H, Ph-*H*), 6.99 (m, 8H, Ph-*H*), 7.27 (m, 8H, Ph-*H*). ¹³C NMR (100 MHz, CD₃CN, ppm): δ 10.38 (Cp*-CH₃), 11.81 (Cp*-CH₃), 41.46 (SCH₂), 42.09 (SCH₂), 95.75 (Cp*-C), 102.94 (Cp*-C), 122.76 (Ph-C), 126.59 (Ph-C), 136.74 (Ph-C). ESI-HRMS (*m/z*): calcd. for 9⁺: 581.0613; found: 581.0615. IR (film, cm⁻¹): 3054, 2981, 2914, 1770, 1479, 1377, 1067, 705, 613. Anal. calcd. for C₄₈H₅₉BFeRuS₃: C, 64.07; H, 6.61. Found: C, 63.93; H, 6.39.

Reaction of 2[PF₆] and thiophenol

An excess of thiophenol (5 μL, 0.048 mmol) was added to a solution of 2[PF₆] (5 mg, 0.007 mmol) in THF-*d*₈ (0.6 mL) at room temperature for about 15 min to give a yellow solution, which was a mixture of complexes 8[PF₆] and 9[PF₆]. ¹H NMR (400 MHz, THF-*d*₈, ppm): δ 1.68, 1.71 (8[PF₆]), -16.81, 1.60, 1.93 (9[PF₆]). ESI-HRMS (*m/z*): found for 8⁺: 689.0648; found for 9⁺: 581.0613.

Conflicts of interest

There are no conflicts to declare.

Acknowledgements

This work was supported by the National Natural Science Foundation of China (No. 21571026, 21690064, and 21231003), the Program for Changjiang Scholars and Innovative Research Team in University (No. IRT13008), and the "111" project of the Ministry of Education of China.

Notes and references

- (a) M. Narayan, E. Welker, W. J. Wedemeyer and H. A. Scheraga, *Acc. Chem. Res.*, 2000, 33, 805–812; (b) G. Bulaj, *Biotechnol. Adv.*, 2005, 23, 87–92; (c) C. W. Gruber, M. Čemažar, B. Heras, J. L. Martin and D. J. Craik, *Trends Biochem. Sci.*, 2006, 31, 455–464; (d) Z. Cheng, J. Zhang, D. P. Ballou and C. H. Williams Jr, *Chem. Rev.*, 2011, 111, 5768–5783; (e) J. Alegre-Cebollada, P. Kosuri, J. A. Rivas-Pardo and J. M. Fernández, *Nat. Chem.*, 2011, 3, 882–887; (f) W. Chen, L. Li, Z. Du, J. Liu, J. N. Reitter, K. V. Mills, R. J. Linhardt and C. Wang, *J. Am. Chem. Soc.*, 2012, 134,

- 2500–2503; (g) T. Ilani, A. Alon, I. Grossman, B. Horowitz, E. Kartvelishvili, S. R. Cohen and D. Fass, *Science*, 2013, **341**, 74–76; (h) M. Góngora-Benítez, J. Tulla-Puche and F. Albericio, *Chem. Rev.*, 2014, **114**, 901–926; (i) A. J. Wommack, J. J. Ziarek, J. Tomaras, H. R. Chileveru, Y. Zhang, G. Wagner and E. M. Nolan, *J. Am. Chem. Soc.*, 2014, **136**, 13494–13497; (j) C. Landeta, J. L. Blazyk, F. Hatahet, B. M. Meehan, M. Eser, A. Myrick, L. Bronstain, S. Minami, H. Arnold, N. Ke, E. J. Rubin, B. C. Furie, B. Furie, J. Beckwith, R. Dutton and D. Boyd, *Nat. Chem. Biol.*, 2015, **11**, 292–298; (k) S. Lu, S.-B. Fan, B. Yang, Y.-X. Li, J.-M. Meng, L. Wu, P. Li, K. Zhang, M.-J. Zhang, Y. Fu, J. Luo, R.-X. Sun, S.-M. He and M.-Q. Dong, *Nat. Methods*, 2015, **12**, 329–331; (l) M. Song, J.-S. Kim, L. Liu, M. Husain and A. Vázquez-Torres, *Cell Rep.*, 2016, **14**, 2901–2911.
- 2 (a) T. T. Conway, E. G. DeMaster, D. J. W. Goon, F. N. Shirota and H. T. Nagasawa, *J. Med. Chem.*, 1999, **42**, 4016–4020; (b) K. C. Nicolaou, R. Hughes, J. A. Pfefferkorn, S. Barluenga and A. J. Roecker, *Chem. – Eur. J.*, 2001, **7**, 4280–4295; (c) S. A. Caldarelli, M. Hamel, J.-F. Duckert, M. Ouattara, M. Calas, M. Maynadier, S. Wein, C. Périgaud, A. Pellet and H. J. Vial, *J. Med. Chem.*, 2012, **55**, 4619–4628; (d) R. V. J. Chari, M. L. Miller and W. C. Widdison, *Angew. Chem., Int. Ed.*, 2014, **53**, 3796–3827; (e) O. Bouteira and G. J. L. Bernardes, *Chem. Rev.*, 2015, **115**, 2174–2195; (f) Q.-Y. Hu, F. Berti and R. Adamo, *Chem. Soc. Rev.*, 2016, **45**, 1691–1719; (g) L. R. Staben, S. G. Koenig, S. M. Lehar, R. Vandlen, D. Zhang, J. Chuh, S.-F. Yu, C. Ng, J. Guo, Y. Liu, A. Fourie-O'Donohue, M. Go, X. Linghu, N. L. Segraves, T. Wang, J. Chen, B. Wei, G. D. L. Phillips, K. Xu, K. R. Kozak, S. Mariathasan, J. A. Flygare and T. H. Pillow, *Nat. Chem.*, 2016, **8**, 1112–1119; (h) M. Feng, B. Tang, S. H. Liang and X. Jiang, *Curr. Top. Med. Chem.*, 2016, **16**, 1200–1216; (i) A. Zorzi, K. Deyle and C. Heinis, *Curr. Opin. Chem. Biol.*, 2017, **38**, 24–29; (j) A. Beck, L. Goetsch, C. Dumontet and N. Corvaia, *Nat. Rev. Drug Discovery*, 2017, **16**, 315–337; (k) D. S. Nielsen, N. E. Shepherd, W. Xu, A. J. Lucke, M. J. Stoermer and D. P. Fairlie, *Chem. Rev.*, 2017, **117**, 8094–8128; (l) Y. Liu, Z. Xie, D. Zhao, J. Zhu, F. Mao, S. Tang, H. Xu, C. Luo, M. Geng, M. Huang and J. Li, *J. Med. Chem.*, 2017, **60**, 2227–2244; (m) J. Mantaj, P. J. M. Jackson, K. M. Rahman and D. E. Thurston, *Angew. Chem., Int. Ed.*, 2017, **56**, 462–488.
- 3 (a) Y. Kishi, T. Fukuyama and S. Nakatsuka, *J. Am. Chem. Soc.*, 1973, **95**, 6492–6493; (b) J. Kim, J. A. Ashenurst and M. Movassaghi, *Science*, 2009, **324**, 238–241; (c) E. Iwasa, Y. Hamashima, S. Fujishiro, E. Higuchi, A. Ito, M. Yoshida and M. Sodeoka, *J. Am. Chem. Soc.*, 2010, **132**, 4078–4079; (d) P. Klausmeyer, S. M. Shipley, K. M. Zuck and T. G. McCloud, *J. Nat. Prod.*, 2011, **74**, 2039–2044; (e) C.-S. Jiang, W. E. G. Müller, H. C. Schröder and Y.-W. Guo, *Chem. Rev.*, 2012, **112**, 2179–2207; (f) K. C. Nicolaou, M. Lu, S. Totokotsopoulos, P. Heretsch, D. Giguère, Y.-P. Sun, D. Sarlah, T. H. Nguyen, I. C. Wolf, D. F. Smee, C. W. Day, S. Bopp and E. A. Winzeler, *J. Am. Chem. Soc.*, 2012, **134**, 17320–17332; (g) P. Chankhamjon, D. Boettger-Schmidt, K. Scherlach, B. Urbansky, G. Lackner, D. Kalb, H.-M. Dahse, D. Hoffmeister and C. Hertweck, *Angew. Chem., Int. Ed.*, 2014, **53**, 13409–13413; (h) M. Feng and X. Jiang, *Chem. Commun.*, 2014, **50**, 9690–9692.
- 4 (a) K. Klesk, M. Qian and R. R. Martin, *J. Agric. Food Chem.*, 2004, **52**, 5155–5161; (b) A. Shimoyama, S. Kido, Y.-I. Kinekawa and Y. Doi, *J. Agric. Food Chem.*, 2008, **56**, 9200–9205; (c) F. S. Hanschen, E. Lamy, M. Schreiner and S. Rohn, *Angew. Chem., Int. Ed.*, 2014, **53**, 11430–11450.
- 5 (a) D. Witt, *Synthesis*, 2008, **16**, 2491–2509; (b) B. Mandal and B. Basu, *RSC Adv.*, 2014, **4**, 13854–13881; (c) J. Yuan, C. Liu and A. Lei, *Org. Chem. Front.*, 2015, **2**, 677–680; (d) M. Wang and X. Jiang, *Top. Curr. Chem.*, 2018, **376**, 1–40.
- 6 (a) C. Liu, H. Zhang, W. Shi and A. Lei, *Chem. Rev.*, 2011, **111**, 1780–1824; (b) C. Liu, J. Yuan, M. Gao, S. Tang, W. Li, R. Shi and A. Lei, *Chem. Rev.*, 2015, **115**, 12138–12204.
- 7 (a) N. Iranpoor and B. Zeynizadeh, *Synthesis*, 1999, **1**, 49–50; (b) S. M. S. Chauhan, A. Kumar and K. A. Srinivas, *Chem. Commun.*, 2003, 2348–2349; (c) J. A. Fernández-Salas, S. Manzini and S. P. Nolan, *Chem. Commun.*, 2013, **49**, 5829–5831; (d) M. Li and J. M. Hoover, *Chem. Commun.*, 2016, **52**, 8733–8736; (e) Y. Dou, X. Huang, H. Wang, L. Yang, H. Li, B. Yuan and G. Yang, *Green Chem.*, 2017, **19**, 2491–2495.
- 8 (a) A. Cervilla, A. Corma, V. Fornés, E. Llopis, P. Palanca, F. Rey and A. Ribera, *J. Am. Chem. Soc.*, 1994, **116**, 1595–1596; (b) A. Dhakshinamoorthy, M. Alvaro and H. Garcia, *Chem. Commun.*, 2010, **46**, 6476–6478; (c) M. Oba, K. Tanaka, K. Nishiyama and W. Ando, *J. Org. Chem.*, 2011, **76**, 4173–4177; (d) A. Corma, T. Ródenas and M. J. Sabater, *Chem. Sci.*, 2012, **3**, 398–404; (e) P. Das, S. Ray, A. Bhaumik, B. Banerjee and C. Mukhopadhyay, *RSC Adv.*, 2015, **5**, 6323–6331.
- 9 (a) A. Hatano, S. Makita and M. Kirihiro, *Bioorg. Med. Chem. Lett.*, 2004, **14**, 2459–2462; (b) R. Dong, M. Pfeiffermann, D. Skidin, F. Wang, Y. Fu, A. Narita, M. Tommasini, F. Moresco, G. Cuniberti, R. Berger, K. Müllen and X. Feng, *J. Am. Chem. Soc.*, 2017, **139**, 2168–2171.
- 10 (a) R. Priefer, Y. J. Lee, F. Barrios, J. H. Wosnick, A.-M. Lebus, P. G. Farrell and D. N. Harpp, *J. Am. Chem. Soc.*, 2002, **124**, 5626–5627; (b) M. H. Ali and M. McDermott, *Tetrahedron Lett.*, 2002, **43**, 6271–6273; (c) E. Bourlès, R. A. de Sousa, E. Galardon, M. Selkti, A. Tomas and I. Artaud, *Tetrahedron*, 2007, **63**, 2466–2471.
- 11 (a) A. R. Hajipour, S. E. Mallakpour and H. Adibi, *J. Org. Chem.*, 2002, **67**, 8666–8668; (b) R. Leino and J.-E. Lönnqvist, *Tetrahedron Lett.*, 2004, **45**, 8489–8491.
- 12 (a) H. Firouzabadi, N. Iranpoor, H. Parham, A. Sardarian and J. Toofan, *Synth. Commun.*, 1984, **14**, 717–723; (b) L. Delaude and P. Laszlo, *J. Org. Chem.*, 1996, **61**, 6360–6370; (c) S. Patel and B. K. Mishra, *Tetrahedron Lett.*, 2004, **45**, 1371–1372.
- 13 (a) C. L. Hill, *Nature*, 1999, **401**, 436–437; (b) T. Punniyamurthy, S. Velusamy and J. Iqbal, *Chem. Rev.*, 2005, **105**, 2329–2363; (c) L. Que, Jr. and W. B. Tolman, *Nature*, 2008, **455**, 333–340; (d) Z. Shi, C. Zhang, C. Tang and N. Jiao, *Chem. Soc. Rev.*, 2012, **41**, 3381–3430.

- 14 (a) D. P. Gamblin, P. Garnier, S. van Kasteren, N. J. Oldham, A. J. Fairbanks and B. G. Davis, *Angew. Chem., Int. Ed.*, 2004, **43**, 828–833; (b) J. L. G. Ruano, A. Parra and J. Alemán, *Green Chem.*, 2008, **10**, 706–711; (c) H. T. Abdel-Mohsen, K. Sudheendran, J. Conrad and U. Beifuss, *Green Chem.*, 2013, **15**, 1490–1495; (d) X.-B. Li, Z.-J. Li, Y.-J. Gao, Q.-Y. Meng, S. Yu, R. G. Weiss, C.-H. Tung and L.-Z. Wu, *Angew. Chem., Int. Ed.*, 2014, **53**, 2085–2089; (e) X. Xiao, M. Feng and X. Jiang, *Chem. Commun.*, 2015, **51**, 4208–4211; (f) A. Talla, B. Driessen, N. J. W. Straathof, L.-G. Milroy, L. Brunsveld, V. Hessel and T. Noël, *Adv. Synth. Catal.*, 2015, **357**, 2180–2186; (g) X. Xiao, M. Feng and X. Jiang, *Angew. Chem., Int. Ed.*, 2016, **55**, 14121–14125; (h) P. Huang, P. Wang, S. Tang, Z. Fu and A. Lei, *Angew. Chem., Int. Ed.*, 2018, **57**, 8115–8119; (i) X. Xiao, J. Xue and X. Jiang, *Nat. Commun.*, 2018, **9**, 2191–2199.
- 15 (a) L. S. Liebeskind, J. Srogl, C. Savarin and C. Polanco, *Pure Appl. Chem.*, 2002, **74**, 115–122; (b) S. Otsuka, H. Yorimitsu and A. Osuka, *Chem. – Eur. J.*, 2015, **21**, 14703–14707.
- 16 (a) J. C. Fontecilla-Camps, P. Amara, C. Cavazza, Y. Nicolet and A. Volbeda, *Nature*, 2009, **460**, 814–822; (b) *Bioinspired Catalysis*, ed. W. Weigand and P. Schollhammer, WileyVCH, Weinheim, 2015.
- 17 (a) B. M. Hoffman, D. Lukoyanov, Z.-Y. Yang, D. R. Dean and L. C. Seefeldt, *Chem. Rev.*, 2014, **114**, 4041–4062; (b) W. Lubitz, H. Ogata, O. Rüdiger and E. Reijerse, *Chem. Rev.*, 2014, **114**, 4081–4148; (c) M. Can, F. A. Armstrong and S. W. Ragsdale, *Chem. Rev.*, 2014, **114**, 4149–4174.
- 18 (a) Y. Chen, Y. Zhou, P. Chen, Y. Tao, Y. Li and J. Qu, *J. Am. Chem. Soc.*, 2008, **130**, 15250–15251; (b) Y. Chen, L. Liu, Y. Peng, P. Chen, Y. Luo and J. Qu, *J. Am. Chem. Soc.*, 2011, **133**, 1147–1149; (c) X. Dong, L. Liu, Y. Zhou, J. Liu, Y. Zhang, Y. Chen and J. Qu, *Dalton Trans.*, 2015, **44**, 14952–14958.
- 19 (a) Y. Li, Y. Li, B. Wang, Y. Luo, D. Yang, P. Tong, J. Zhao, L. Luo, Y. Zhou, S. Chen, F. Cheng and J. Qu, *Nat. Chem.*, 2013, **5**, 320–326; (b) X. Ji, P. Tong, D. Yang, B. Wang, J. Zhao, Y. Li and J. Qu, *Dalton Trans.*, 2017, **46**, 3820–3824; (c) Y. Zhang, T. Mei, D. Yang, Y. Zhang, B. Wang and J. Qu, *Dalton Trans.*, 2017, **46**, 15888–15896.
- 20 (a) D. Yang, Y. Li, L. Su, B. Wang and J. Qu, *Eur. J. Inorg. Chem.*, 2015, **2015**, 2965–2973; (b) X. Ji, D. Yang, P. Tong, J. Li, B. Wang and J. Qu, *Organometallics*, 2017, **36**, 1515–1521; (c) Y. Zhang, P. Tong, D. Yang, J. Li, B. Wang and J. Qu, *Chem. Commun.*, 2017, **53**, 9854–9857; (d) X. Zhao, D. Yang, Y. Zhang, B. Wang and J. Qu, *Chem. Commun.*, 2018, **54**, 11112–11115.
- 21 (a) Y. Tao, B. Wang, B. Wang, L. Qu and J. Qu, *Org. Lett.*, 2010, **12**, 2726–2729; (b) Y. Tao, B. Wang, J. Zhao, Y. Song, L. Qu and J. Qu, *J. Org. Chem.*, 2012, **77**, 2942–2946; (c) X. Zhao, D. Yang, Y. Zhang, B. Wang and J. Qu, *Org. Lett.*, 2018, **20**, 5357–5361.
- 22 B. Steinmetz and W. A. Schenk, *Organometallics*, 1999, **18**, 943–946.
- 23 Y. Li, Y. Zhang, D. Yang, Y. Li, P. Sun, B. Wang and J. Qu, *Organometallics*, 2015, **34**, 1661–1667.
- 24 (a) P. Sun, D. Yang, Y. Li, Y. Zhang, L. Su, B. Wang and J. Qu, *Organometallics*, 2016, **35**, 751–757; (b) Y. Zhang, D. Yang, Y. Li, B. Wang, X. Zhao and J. Qu, *Dalton Trans.*, 2017, **46**, 7030–7038.
- 25 Y. Zhang, D. Yang, Y. Li, X. Zhao, B. Wang and J. Qu, *Organometallics*, 2018, **37**, 3165–3173.
- 26 U. Kölle, F. Khouzami and B. Fuss, *Angew. Chem., Int. Ed. Engl.*, 1982, **21**, 131–132.
- 27 D. Catheline and D. Astruc, *J. Organomet. Chem.*, 1983, **248**, C9–C12.
- 28 D. Catheline and D. Astruc, *Organometallics*, 1984, **3**, 1094–1100.
- 29 (a) D. Yang, Y. Li, B. Wang, X. Zhao, L. Su, P. Tong, Y. Luo and J. Qu, *Inorg. Chem.*, 2015, **54**, 10243–10249; (b) Y. Zhang, J. Zhao, D. Yang, Y. Zhang, B. Wang and J. Qu, *Inorg. Chem. Commun.*, 2017, **83**, 66–69.
- 30 S. Venkataramani, U. Jana, M. Dommaschk, F. D. Sönnichsen, F. Tuczek and R. Herges, *Science*, 2011, **331**, 445–448.
- 31 M. Yuki, Y. Miyake and Y. Nishibayashi, *Organometallics*, 2010, **29**, 5994–6001.
- 32 P. Tong, W. Xie, D. Yang, B. Wang, X. Ji, J. Li and J. Qu, *Dalton Trans.*, 2016, **45**, 18559–18565.
- 33 (a) S. Cai, X.-F. Hou, Y.-Q. Chen and G.-X. Jin, *Dalton Trans.*, 2006, 3736–3741; (b) M. Murata, S. Habe, S. Araki, K. Namiki, T. Yamada, N. Nakagawa, T. Nankawa, M. Nihei, J. Mizutani, M. Kurihara and H. Nishihara, *Inorg. Chem.*, 2006, **45**, 1108–1116; (c) H. Gao, J. Huang, L. Chen, R. Liu and J. Chen, *RSC Adv.*, 2013, **3**, 3557–3565; (d) M. E. Carroll, J. Chen, D. E. Gray, J. C. Lansing, T. B. Rauchfuss, D. Schilter, P. I. Volkers and S. R. Wilson, *Organometallics*, 2014, **33**, 858–867; (e) P. Ghosh, M. Quiroz, N. Wang, N. Bhuvanesh and M. Y. Darensbourg, *Dalton Trans.*, 2017, **46**, 5617–5624.
- 34 P. Buchwalter, J. Rosé and P. Braunstein, *Chem. Rev.*, 2015, **115**, 28–126.
- 35 P. Anastas and N. Eghbali, *Chem. Soc. Rev.*, 2010, **39**, 301–312.
- 36 (a) A. K. Justice, R. C. Linck, T. B. Rauchfuss and S. R. Wilson, *J. Am. Chem. Soc.*, 2004, **126**, 13214–13215; (b) M. A. Alvarez, M. E. García, D. García-Vivó, E. Huergo and M. A. Ruiz, *Inorg. Chem.*, 2018, **57**, 912–915.
- 37 M. Yuki, K. Sakata, Y. Hirao, N. Nonoyama, K. Nakajima and Y. Nishibayashi, *J. Am. Chem. Soc.*, 2015, **137**, 4173–4182.
- 38 (a) T. Iwasa, H. Shimada, A. Takami, H. Matsuzaka, Y. Ishii and M. Hidai, *Inorg. Chem.*, 1999, **38**, 2851–2859; (b) M. Gargir, Y. Ben-David, G. Leituss, Y. Diskin-Posner, L. J. W. Shimon and D. Milstein, *Organometallics*, 2012, **31**, 6207–6214.
- 39 C. M. Fendrick, L. D. Schertz, E. A. Mintz, T. J. Marks, T. E. Bitterwolf, P. A. Horine, T. L. Hubler, J. A. Sheldon and D. D. Belin, *Inorg. Synth.*, 1992, **29**, 193–198.
- 40 P. A. Ulmann, A. B. Braunschweig, O.-S. Lee, M. J. Wiester, G. C. Schatz and C. A. Mirkin, *Chem. Commun.*, 2009, 5121–5123.
- 41 U. Jahn, P. Hartmann, I. Dix and P. G. Jones, *Eur. J. Org. Chem.*, 2001, **2001**, 3333–3335.

- 42 L. Y. Goh, M. E. Teo, S. B. Khoo, W. K. Leong and J. J. Vittal, *J. Organomet. Chem.*, 2002, **664**, 161–169.
- 43 G. M. Sheldrick, *SADABS, Program for area detector adsorption correction*, Institute for Inorganic Chemistry, University of Göttingen, Germany, 1996.
- 44 G. M. Sheldrick, *SHELXL-2014, Program for refinement of crystal structures*, University of Göttingen, Germany, 2014; G. M. Sheldrick, *SHELXS-2014, Program for Solution of Crystal Structures*, University of Göttingen, Germany, 2014.